Effective design and operation strategy of renewable cooling and heating system for building application in hot-humid climate

Fong, K.F.; Lee, C.K.; Zhao, T.F.

Published in:
Solar Energy

Published: 01/02/2017

Document Version:
Post-print, also known as Accepted Author Manuscript, Peer-reviewed or Author Final version

Published version (DOI):
10.1016/j.solener.2016.12.045

Publication details:
Fong, K. F., Lee, C. K., & Zhao, T. F. (2017). Effective design and operation strategy of renewable cooling and heating system for building application in hot-humid climate. *Solar Energy*, *143*, 1-9. https://doi.org/10.1016/j.solener.2016.12.045

Effective design and operation strategy of renewable cooling and heating system for building application in hot-humid climate

K.F. Fong[1,*], C.K. Lee[1], T.F. Zhao[2]

[1]Division of Building Science and Technology, College of Science and Engineering, City University of Hong Kong, Hong Kong, China

[2]Department of Architecture and Civil Engineering, College of Science and Engineering, City University of Hong Kong, Hong Kong, China

*Corresponding author.

Tel: 852-3442-8724, fax: 852-3442-0443

Email address: bssquare@cityu.edu.hk

Post address: Tat Chee Avenue, Kowloon, Hong Kong, China

http://dx.doi.org/10.1016/j.solener.2016.12.045

Abstract

The utilization of renewable energy sources is commonly constrained by the building form and the site environment particularly in a densely-populated city which limits the space available to install the respective facilities. The hybrid use of solar and geothermal energy helps improve the situation as the roof and the ground can be fully utilized. A renewable cooling and heating system (RCHS) was therefore investigated based on this approach when applied to a three-storey office building in sub-tropical climate. Solar energy was used in absorption cooling and water heating while ground source was utilized by a high-temperature chiller for radiant cooling. Appropriate control and operation schemes were adopted for the ground-coupled radiant cooling system according to the ambient conditions in order to minimize the system energy demand. By performing dynamic system simulations using TRNSYS, the year-round performances of RCHS were thoroughly evaluated under different design factors including radiant panel type, ground thermal conductivity, borehole length and water heating demand. It was found that the RCHS was effective to tackle the high cooling demand for building in the hot-humid climate, with 44.4% annual primary energy saving against the conventional system.

Keywords: Renewable cooling and heating; solar energy; ground source; control and operation.

1. Introduction

Renewable energy becomes an essential player for climate change mitigation (IPCC, 2011). In a modern city, buildings contribute to the majority of the energy demand. In particular the heating, ventilation and air-conditioning (HVAC) as well as the water heating systems account for over half of the building energy use. Hence, the adoption of renewable cooling and heating in buildings is essential to relieve the climate change. To achieve this, solar thermal energy has been advocated for heating and cooling in the recent decade in regions with mild summer and cold winter. The various solar cooling and heating technologies for use in buildings were outlined (Eicker, 2003 & 2009; Henning 2004). A novel building-integrated solar cooling and heating system was investigated for use in Tianjin with the average cooling capacity reaching 87 W/m^2 in summer (Cui et al., 2015). Analysis was made on solar cooling systems installed in different climatic conditions (Eicker et al., 2015). It was found that the primary energy saving was between 30 to 79%, and to achieve a payback period of 10 years the investment cost had to be reduced by 30 to 70%. A multi-objective design optimization methodology was proposed and applied to an integrated solar absorption cooling and heating system for use in an office building in various cities of USA in terms of the economic, energy and environmental merits. Meanwhile, the use of ground-source heat pump (GSHP) system has been popular for space cooling and heating in Europe and USA. Design and installation guidelines for the GSHP systems were proposed (CIBSE, 2013; Kavanaugh and Rafferty, 2014). The application of GSHP systems for cooling and heating in a district level of different European countries was investigated (De Carli et al., 2014) with the primary energy saving between 50 to 80%. A GSHP system with horizontal ground heat exchangers was tested and used to validate a simulation model in TRNSYS for system control optimization study (Safa et al., 2015) with an energy saving of 28.2% achieved.

In recent years, the European Technology Platform on Renewable Heating and Cooling aims at decarbonization of the energy sector through the effective deployment of renewable energy sources for heating and cooling (2020-2030-2050 Common Vision for the Renewable Heating & Cooling Sector in Europe, 2011; Common Implementation Roadmap for Renewable Heating and Cooling Technologies, 2014). To achieve the goal, it is expected that the involvement of more than one renewable source is necessary in order to maximize the provision of renewable energy for generating the approach of "renewable heating and cooling". In the urban areas, the combined use of solar energy and geothermal energy is worth being promoted, particularly to the multi-storey buildings with severe space constraints in which usually only the roof and the ground are available to install the renewable energy systems. Indeed, from a previous study by the authors (Fong et al., 2010a), the use of the roof for installing the solar collectors could only manage to serve the cooling load for one office floor when applied to sub-tropical climate. Hence, full utilization of both the roof and the ground within the building site is important in this circumstance.

The common design for the combined use of solar thermal energy and geothermal source employs solar heat to relieve the load deficit in the ground when applied to heating-dominated regions. This is directed to the development of solar-assisted ground source heat pump (SAGSHP) systems, which were found with tangible energy merit in space heating and water heating compared to the conventional provision. The performance of a SAGSHP system for use in a greenhouse in Turkey was experimentally investigated (Ozgener and Hepbasli, 2005). It was found that auxiliary heating source was required to maintain the greenhouse temperature in winter. The combined use of GSHP and SAGSHP systems in an office building in Tianjin was analyzed by dynamic simulation using TRNSYS (Wang et al., 2012). An energy saving of 32% could be achieved. A laboratory scale SAGSHP installed in Dalian was studied experimentally under different operating modes (Dai et al., 2015). It was found that the connection of the hot water tank in series with the ground heat exchangers was recommended for use in the coldest month in Dalian. The performance of a SAGSHP was investigated by dynamic system simulation for use in a heating-dominated city in Canada (Rad et al., 2013). It was found that the adoption of the SAGSHP system could reduce the overall length of the ground heat exchangers by 15% as compared to those which employed a conventional GSHP system. Comprehensive experimental investigation and analysis of a SAGSHP system was conducted for four heating modes of operation (Yang et al. 2015). The average coefficient of performance under the various heating modes was 50% and 31%

higher than those based on the GSHP system and solar-assisted heat pump system. A novel SAGSHP system was designed to provide space cooling/heating and water heating for an office building in Beijing (Si et al. 2014). Operation strategies were developed and design optimization was made through dynamic simulation using TRNSYS. It was found that the connection of the solar collectors in series with the ground heat exchangers performed better as reflected by a smaller soil temperature drop after 10 years of operation. Optimization of a SAGSHP system for use in India was carried out by two optimization methods (Verma and Murugesan, 2014). The optimum coefficient of performance was found to be 4.23. The application of SAGSHP systems in 19 European cities were investigated (Girard et al., 2015). The average system coefficient of performance ranged from 4.4 to 5.8 while it was between 4.3 and 5.1 for conventional GHSP systems. The payback periods varied from 8.5 to 23 years with better performance in southern Europe. Performance comparison of a SAGSHP system was also made by using R22 and R744 as refrigerants for the heat pump. It was found that the energy performance of the heat pump was 28.8% higher with the use of R22 and that the heating capacity of the heat pump with R22 was 10% higher than that based on R744. Meanwhile, the solar collector efficiency was 4.1% higher with the employment of R744.

Besides the common design of SAGSHP system as mentioned before, the ground heat exchangers can be coupled with the cooling tower in a solar cooling system to enhance the system efficiency. A case study was made in Spain in which cooled groundwater at around 22 °C from one ground well was drawn to assist the cooling tower in cooling the condenser water supplied to a solar-driven absorption chiller (Rosiek and Batlles, 2012). The warmed groundwater was discharged back to the ground through another ground well. It was found that 31% of the electric demand from the cooling tower could be saved and that the water consumption from the cooling tower reduced by 116 m^3.

However, in a hot and humid city in which the annual air-conditioning load is cooling-dominated, such kind of common solar-assisted ground-source system design is considered inappropriate. In particular, air-conditioning is indispensable in office buildings throughout the year, whereas heating demand is comparatively minimal. Practical considerations like architectural geometry, site environment and space availability of the building also substantially affect the amount of renewable energy that can be harnessed. As a result, this study is to devise a more effective design and operation strategy for the renewable cooling and heating system (RCHS) utilizing both solar energy and ground source, with emphasis on serving multi-storey building under hot-humid climate.

2. System design and operation of renewable cooling and heating

2.1 Design of RCHS

The proposed RCHS was formulated with the composition of solar absorption cooling and ground-source radiant cooling to share the total system cooling load (i.e. the sum of zone load and ventilation load) for an office building, as shown in Fig. 1. A water-cooled LiBr-H_2O absorption chiller, which utilized the solar heat collected from the solar panels, was employed to supply chilled water to cool the fresh or supply air by a chilled water pump (EWP) through an air-handling unit which consisted of a supply air coil and a supply air fan (SAF). A three-way supply air valve (SAV) was fitted to control the chilled water flow rate to the supply air coil. A cooling water pump (CWP) was used to transport the condenser water from a cooling tower to the absorption chiller. Meanwhile, a high-temperature vapor-compression chiller, with the design chilled water temperature higher than that conventionally used, was used to supply high-temperature chilled water to the radiant panels by a radiant panel pump (RPP) and to reject heat to the ground by a borefield water pump (BWP) during the peak-load period. The water flow to the radiant panels was controlled by a three-way radiant panel valve (RPV). With a higher coefficient of performance (*COP*) offered by the high-temperature chiller, the required depth for the vertical ground heat exchanger (GHE) could thus be minimized. The use of radiant cooling also reduced the power demand from the supply air fan. The high-temperature chiller was therefore designed to serve the zone sensible load, while the absorption chiller was used to handle the remaining cooling load. To further enhance the energy merit of the proposed system, the high-temperature chiller would be switched off and the GHE was directly coupled to the radiant panels during the low-load period as described in details in Section 2.2. Two free cooling valves (FCV1 and FCV2) were installed in order to allow the water to flow directly from the GHE to radiant panels.

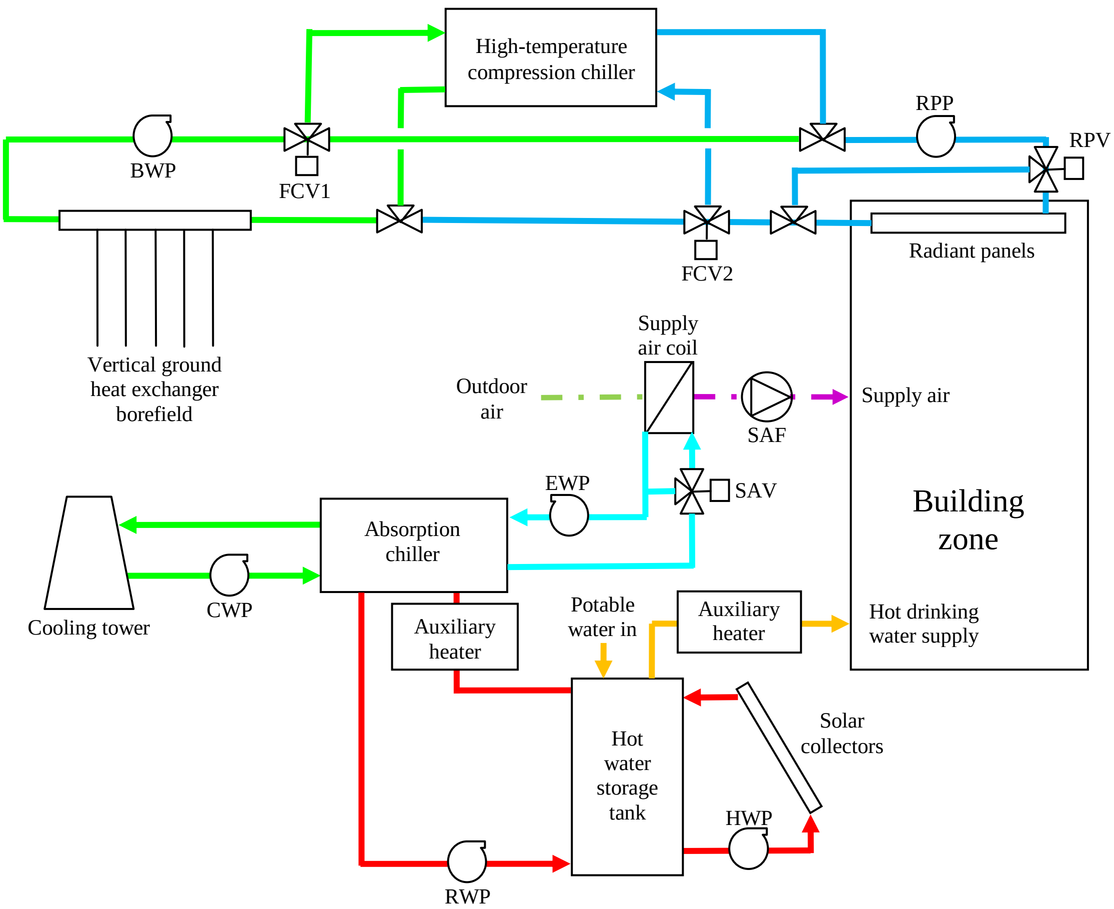

Fig. 1. Schematic diagram of the ground-assisted solar cooling and heating system for a three-storey office building.

The evacuated tubes were employed as the solar collectors. A hot water pump (HWP) was used to convey the solar heat from the solar collector to a hot water storage tank. A regenerative water pump (RWP) was then employed to circulate the hot water between the hot water tank and the absorption chiller. An auxiliary heater was used for the absorption chiller in case the solar thermal gain was not sufficient. For the radiant panels, both the chilled ceiling (CC) and the passive chilled beams (PCB) were considered in this study. For an office building in a hot-humid city, space heating is rather insignificant but hot drinking water is generally provided in the pantries. Therefore in the RCHS, the hot water storage tank of the solar thermal system was also used to pre-heat the potable water for drinking purpose. Another auxiliary heater was furnished in order to raise the hot water temperature up to the boiling point when necessary.

2.2 Control and operation of RCHS

In order to enhance system efficiency, the RCHS was designed with an appropriate control and operation scheme, which consisted of the following three operation modes according to the ambient conditions:

- Mode 1 involved the simultaneous functioning of the absorption chiller and the high-temperature chiller. This occurred when the ambient temperature was above 20 °C.
- Mode 2 operated when the ambient temperature was between 15 °C and 20 °C. In this situation, the high-temperature chiller stopped with only the absorption chiller functioned and the GHE was directly coupled to the radiant panels.
- Mode 3 was activated when the ambient temperature fell below 15 °C, in which the absorption chiller also stopped. The system was then operating in a free-cooling mode by radiant panels and the untreated outdoor air only.

The selection of the respective temperature ranges for Modes 2 and 3 was not arbitrary, but based on repeated trials through dynamic system simulations in order that the zone temperature under Modes 2 and 3 would not exceed 27 °C within the daily operation schedule of the system. Actually both Modes 2 and 3 fully utilized the renewable energy sources of solar energy and ground source to provide cooling and water heating for building use when the climatic conditions were appropriate, especially out of the summer period.

2.2.1 Mode 1

The supply air valve was controlled by two proportional controllers which monitored the zone temperature and humidity ratio. The respective minimum/maximum setpoints for the temperature and humidity ratio controllers were 24.5 °C/26.5 °C and 0.01235/0.0125. The maximum signal from the two controllers was used to activate the supply air valve. This was necessary in order to maintain the zone humidity at the design level, or the radiant panels would have condensation risk. The operations of the absorption chiller, regenerative water pump and cooling water pump were controlled by a return chilled water thermostat between 9 and 12 °C. The functioning of the cooling tower was additionally governed by the return cooling water thermostat between 15 and 20 °C when the absorption chiller was running.

The high-temperature chiller was controlled by a thermostat between 20 and 23°C according to the water temperature returning from the radiant panels. The two free cooling valves were closed which separated the water flows between the GHE and the radiant panels. To minimize the risk of condensation on the radiant panel surface, a dew controller was used which stopped the high-temperature chiller when the water temperature entering the radiant panels was lower than the zone dewpoint. The borefield water pump functioned when the high-temperature chiller started. The radiant panel valve was controlled linearly by the same room temperature controller as for the supply air valve. To ensure that cooling was provided by the radiant panels, the radiant panel valve was additionally governed by a differential thermostat between 0 and 3 °C which monitored the temperature surplus between the building zone and the water entering the radiant panels. The supply air fan, chilled water pump and radiant panel pump ran continuously throughout the entire daily operating schedule.

2.2.2 Mode 2

The high-temperature chiller was disabled. The two free-cooling valves opened which bypassed the water from the high-temperature chiller. In this regard, the borefield water was pumped directly into the radiant panels and then returned back to the GHE. The borefield water pump and radiant panel pumps were energized when the signal from the temperature controller for the supply air valve was greater than zero and the radiant panel valve opened fully in this situation. The operations of the absorption chiller plant and the supply air system were the same as those in Mode 1.

2.2.3 Mode 3

Both the absorption chiller plant and the high-temperature chiller were stopped. The supply air valve was also closed. Only the supply air fan remained in operation. The ground-coupled radiant cooling system functioned in the same way as that in Mode 2.

3. Specifications of RCHS and building zone

In this study, the RCHS was applied to a three-storey office building in the subtropical Hong Kong (22.3°N and 114.2°E) with 196 m^2 on each floor under a daily occupying schedule from 8:00 a.m. to 6:00 p.m. The three floors were identical in plan arrangement, occupancy and functional use. The design criteria of load calculation are summarized as follows:

- Design indoor conditions: 25.5 °C and 60% relative humidity (RH)
- Total floor area: 588 m^2
- Maximum number of office occupant: 24/floor
- Sensible heat gain of occupant: 65 W/occupant (seated with very light writing)
- Latent heat gain of occupant: 55 W/occupant (seated with very light writing)
- Heat gains of lighting: 17 W/m^2
- Heat gains of office equipment: 25 W/m^2
- Outdoor air requirement: 0.01 m^3/s per occupant

The zone cooling demand was determined by using a component-based simulation platform (TRNSYS, 2006) and its component library (TESS, 2006) under the typical meteorological year (TMY) of Hong Kong (Chan et al., 2006). Fig. 2 shows the average total solar insolation within the daily operating schedule on a horizontal plane in the TMY.

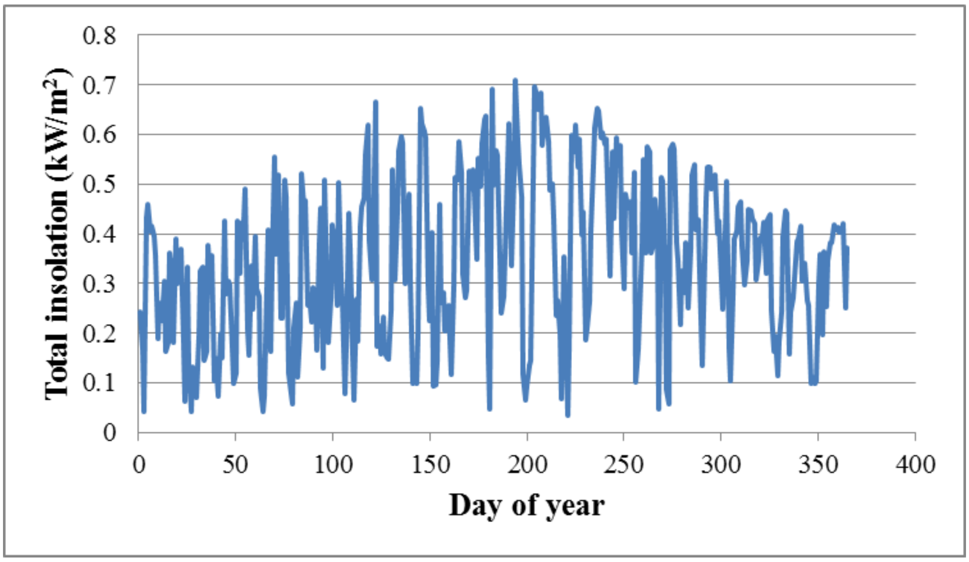

Fig. 2. Year-round profile of the daily-averaged total insolation on a horizontal plane in the TMY of Hong Kong.

Each piece of equipment in a system was represented by a component in TRNSYS with specified input and outputs. TRNSYS offered an interactive interface to add and link up the components as desired in order to build the system. At each simulation time step, the inputs and outputs of all the components were calculated in a closed-loop manner iteratively until convergence was met. TRNSYS provided many standard components which were required to build a system and it also allowed the users to develop their own components. Table 1 shows the simulated building loads for the three floors. The total system cooling load (zone load plus ventilation load) was 87 kW for the office building. The required capacity of the high-temperature chiller (serving the zone sensible load only) became 48 kW for three floors, and the absorption chiller was used to handle the remaining 39 kW.

Table 1. Summarized design building loads and chiller capacities for the office building.

Load type	Value
Zone load (Sensible / latent) (kW)	48 / 9
Ventilation load (Sensible / latent) (kW)	9 / 21
System load (Sensible / latent) (kW)	57 / 30
Design capacity of high-temperature chiller (kW)	48
Design capacity of absorption chiller (kW)	39

The design entering regenerative, cooling and chilled water temperatures for the absorption chiller were 90 °C, 30 °C and 13 °C respectively. For the high-temperature vapor-compression chiller, selection of the various parameters was based the normal return chilled water temperature of 13 °C at a *COP* of 3. In the operation of the high-temperature vapor-compression chiller, the design return chilled water temperature was 22 °C. Hence, the design *COP* would rise to 3.4. To allow for the direct coupling between the GHE and the radiant panels in Modes 2 and 3, the flow rates of the borefield water pump and radiant panel pump were taken to be the same. The design temperature drop for the chilled water was 3 °C across the high-temperature chiller, since it was constrained by both the design zone temperature and the zone dew point temperature. The models developed in a previous study by the authors (Fong et al., 2012) were employed to determine the performance of the absorption and vapor-compression chiller. New TRNSYS components were developed for both types of chillers. Performance data files at different operating conditions were generated using the models mentioned in Fong et al. (2012), and the new TRNSYS components determined the chiller performance simply by multi-dimensional linear interpolation using the generated performance data files.

For the CC and the PCB, the configurations and modeling approaches used in another previous study by the authors (Fong et al., 2010b) were adopted. A built-in active layer embedded in the building zone component of TRNSYS was employed to model the CC. Meanwhile, another new TRNSYS component was created for the PCB which calculated the capacity of the PCB based on the performance curves from one supplier (Carrier, 2008). The efficiency coefficients determined from a test report (Hochschul Rapperswil of Switzerland, 1997) were used for the evacuated tubes. The allowable solar collector area and borefield configuration were constrained by the roof area and the site boundary respectively. As a typical multi-storey building, the roof area or the site area was taken same as the floor area of 196 m^2. The total area of the solar collectors was 100 m^2, and the size of the hot water storage tank was 5 m^3. For the vertical ground heat exchanger borefield, a new TRNSYS component model was also developed based on a 3-D numerical model (Lee and Lam, 2008). A closed system was employed in which the borefield water circulated through vertical U-tubes installed inside each borehole and backfilled by a thermally-enhanced grout. No groundwater effect was taken into account. For all TRNSYS standard components, default parameters were applied unless otherwise specified. Table 2 summarizes all the major parameter values used for the RCHS in this study.

Table 2. Design parameters used for RCHS.

Parameter	Value
Supply air stream	
Supply air volume flow rate ($m^3 \cdot s^{-1}$)	0.24
Supply air fan power (kW)	0.257
Absorption Chiller	
Regenerative / cooling / chilled water mass flow rate ($kg \cdot s^{-1}$)	2.7 / 4.8 / 1.9
Overall heat transfer value ($kW \cdot K^{-1}$)	
Generator / absorber / condenser / evaporator	6.3 / 6.3 / 6.3 / 5.3
Solution-to-solution heat exchanger	1.3

Degree of superheat at evaporator outlet (°C)	5.0
Solution volume flow rate at absorber outlet ($l \cdot s^{-1}$)	0.15
Cooling water system	
Cooling tower air volume flow rate ($m^3 \cdot s^{-1}$)	3.61
Cooling tower fan power (kW)	1.111
Cooling water pump power (kW)	1.024
Chilled water system	
Chilled water pump power (kW)	0.437
Hot water system	
Hot water mass flow rate ($kg \cdot s^{-1}$)	2.7
Hot / regenerative water pump power (kW)	0.216 / 0.328
High-temperature chiller (for each floor)	
Borefield / radiant panel water mass flow rate ($kg \cdot s^{-1}$)	1.5 / 1.5
Overall heat transfer value of condenser / evaporator ($kW \cdot K^{-1}$)	1.8 / 1.3
Volume of refrigerant in condenser / evaporator / liquid line (litre)	3 / 3 / 0.015
Refrigerant mass (kg)	1.97
Degree of superheat at compressor suction (°C)	11.1
Radiant panel pump power (kW)	1.8
Ground heat exchanger borefield	
Borefield configuration	3 x 3
Borehole separation (m)	4.5
Borehole radius (m)	0.055
Insulated length of borehole (m)	5
Number of U-tube inside each borehole	2
Tube inner / outer radius (m)	0.013 / 0.016
Distance of tube centre from borehole centre (m)	0.03
Ground / pipe / grout thermal conductivity ($W \cdot m^{-1} \cdot K^{-1}$)	3.5 / 0.4 / 1.3
Ground volumetric heat capacity ($kJ \cdot m^{-3} \cdot K^{-1}$)	2160

4. Methodology of analysis

In order to evaluate the system performance under the changing loading and climatic conditions, dynamic simulation was carried out using TRNSYS for one year based on the typical weather data of Hong Kong and a simulation time step of 3 minutes was applied. Respective operating data were recorded in files during the course of the simulation for further evaluation of the system performance.

As solar energy was involved, the effectiveness of the RCHS was represented by the solar fraction (*SF*) defined as

$$SF = \frac{\text{Solar energy}}{\text{Solar energy} + \text{auxiliary heat energy}} \quad (1)$$

SF measured the portion of the driving energy that came from the solar energy system, and a high *SF* means that a lower proportion of the driving energy was provided by the auxiliary energy source.

To investigate the energy-saving potential of the RCHS clearly, primary energy analysis would be made. All parasitic energy consumptions from the pumps, the fans, the cooling tower and sundry items were accounted for. An energy efficiency of 33% was assumed for the electric power plant in relation to the primary energy input. The auxiliary heater was assumed to be run directly on primary energy with a combustion efficiency of 90%. The water-cooled vapor-compression chiller (WCVCC) would be used as a base case for performance benchmarking. The year-round system performance of the RCHS at different types of radiant panels, ground thermal conductivities, lengths of borehole and water heating demand was then analyzed.

5. Results and discussions

5.1 Effect of radiant panels on cooling performance

Table 3 summarizes the year-round cooling performances of the RCHS for the two types of radiant panels. The selected lengths for the boreholes were based on a maximum borefield fluid leaving temperature ($T_{bf,out,max}$) of around 29 °C. Clearly, the use of PCB offered a better system performance in terms of the averaged zone conditions and the total primary energy consumption as compared to that using CC. In view of the indoor temperature, the RCHS using CC had the problem of thermal comfort according to the design temperature of 25.5 °C. The much higher radiative load ratio of CC as compared to that for PCB necessitated far longer operation of the high-temperature chiller and the absorption chiller, since the radiative load was not effective in reducing the zone temperature. This resulted RCHS-CC in much longer boreholes to be used and substantially greater primary energy consumption. This also explains why the *SF* decreased in the case using CC.

Table 3. Comparison of year-round performances of RCHS using different radiant panels.

System	*SF*	$T_{zone,avg}$ (°C)	$RH_{zone,avg}$ (%)	Primary energy consumption (kWh)	Borehole length (m)	Water consumption of cooling tower (m^3)
RCHS-CC	0.543	27.0	46.1	215,546	200	256.8
RCHS-PCB	0.656	25.0	59.6	124,113	140	200.8
WCVCC	NA	24.8	58.9	223,293	NA	82.2

Remark: NA refers to not applicable.

The year-round total primary consumption for the WCVCC system was based on 74,431 kWh per floor in the previous study (Fong et al., 2011). Therefore the energy-saving potential of the RCHS using PCB would be 44.4%. Although the RCHS using CC had slightly lower energy consumption than the WCVCC, it had a fatal problem of not providing satisfactory indoor temperature in general. As a result, the RCHS using PCB would be an appropriate choice in the system design. Meanwhile, the proportion of running times or run fractions of the RCHS operating in Modes 1, 2 and 3 were 71.9, 21.7 and 6.4% respectively. This meant that in 28.1% of the system operating times, the high-temperature chiller was not needed.

From Table 3, the water consumption of the cooling tower was much higher with the employment of the RCHS system. This could be explained by the substantially lower *COP* of the absorption chiller as compared to that of the conventional WCVCC which necessitated the use of a cooling tower with a much higher capacity and condenser water flow rate even though the capacity of the absorption chiller was 55% lower than that of the WCVCC. Indeed, the power consumption from the cooling tower and the cooling water pump was also higher with the employment of the RCHS.

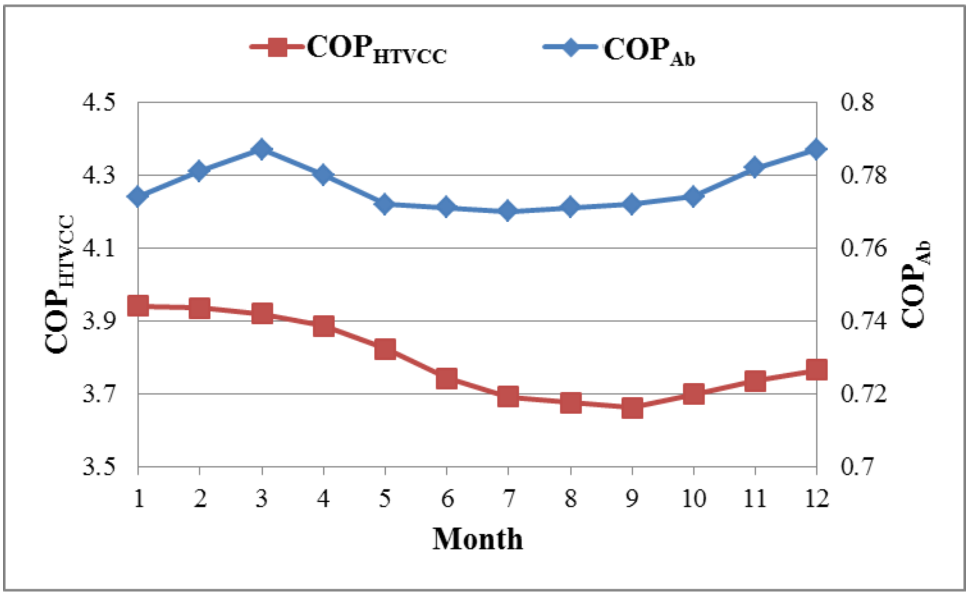

Fig. 3. Profiles of monthly averaged *COP's* of the absorption and high-temperature vapor-compression chillers for the RCHS-PCB system

Fig. 3 depicted the profiles of the monthly-averaged *COP's* for the absorption and high-temperature chillers in the RCHS-PCB system. *COP* of absorption chiller (COP_{Ab}) and *COP* of high-temperature vapor-compression chiller (COP_{HTVCC}) are defined as follows:

$$COP_{Ab} = \frac{\text{Cooling capacity}}{\text{Heat input to generator}} \tag{2}$$

$$COP_{HTVCC} = \frac{\text{Cooling capacity}}{\text{Electricity input to compressor}} \tag{3}$$

The year-round fluctuation of the *COP* of the absorption chiller was much less than that of the high-temperature chiller. With elevated chilled water supply temperature, the resulting *COP* of the high-temperature chiller was around 3.8, which was substantially higher than that of 3 for a conventional design. This highlighted the merit of the proposed RCHS system in which the energy performance of the employed equipment was fully enhanced.

5.2 Effect of ground thermal conductivity and length of borehole on system design and performance

With the choice of PCB for the RCHS, the borehole length would be 140 m in this study. So far, the design thermal conductivity was a favorable value of 3.5 W/mK. If the thermal conductivity of the actual ground material was lower, there would be impact on the required borehole length and the fluid temperature leaving the GHE. To investigate this, various ground thermal conductivities were attempted under two circumstances, the first one with the same borehole length while the second one with approximately the same design $T_{bf,out,max}$. Table 4 summarizes the results of such parametric study.

Table 4. Comparison of year-round performances of RCHS at different ground thermal conductivities and lengths of borehole.

Ground thermal conductivity (W/mK)	Length of borehole (m)	*SF*	$T_{zone,avg}$ (°C)	$RH_{zone,avg}$ (%)	Primary energy consumption (kWh)	$T_{bf,out,max}$ (°C)
3.5	140	0.656	25.00	59.60	124,113	29.00
3.0	140	0.657	24.97	59.57	124,289	29.71
3.0	150	0.658	24.96	59.62	123,272	29.00
2.5	140	0.655	24.98	59.50	124,100	30.58
2.5	162	0.654	24.97	59.62	123,598	29.03
2.0	140	0.655	25.00	59.41	125,756	31.69
2.0	178	0.653	24.97	59.61	124,146	29.04

With the same borehole length of 140 m, the year-round total primary energy consumption was increased by 1.3% when the ground thermal conductivity decreased by 42.9%, i.e. from 3.5 down to 2.0 W/mK. However, $T_{bf,out,max}$ rose by 9.3% from 29 °C to 31.69 °C correspondingly, as illustrated in Fig. 4. As the ground temperature increased with time, $T_{bf,out,max}$ was expected to be even higher in the long term, this would gradually reduce the energy efficiency of the system in the subsequent years of operation. If $T_{bf,out,max}$ was kept at the level of 29 °C, the required borehole length would be increased by 27.1% and up to 178 m, when the ground thermal conductivity dropped to 2.0 W/mK, as depicted in Fig. 5. From both Figs. 4 and 5, it is observed that the increasing trends of borefield fluid leaving temperature and borehole length are not linear, but slightly bent up in the drop of ground thermal conductivity. This indicates that the ground or soil thermal property is vital to offer satisfactory year-round performance of the RCHS.

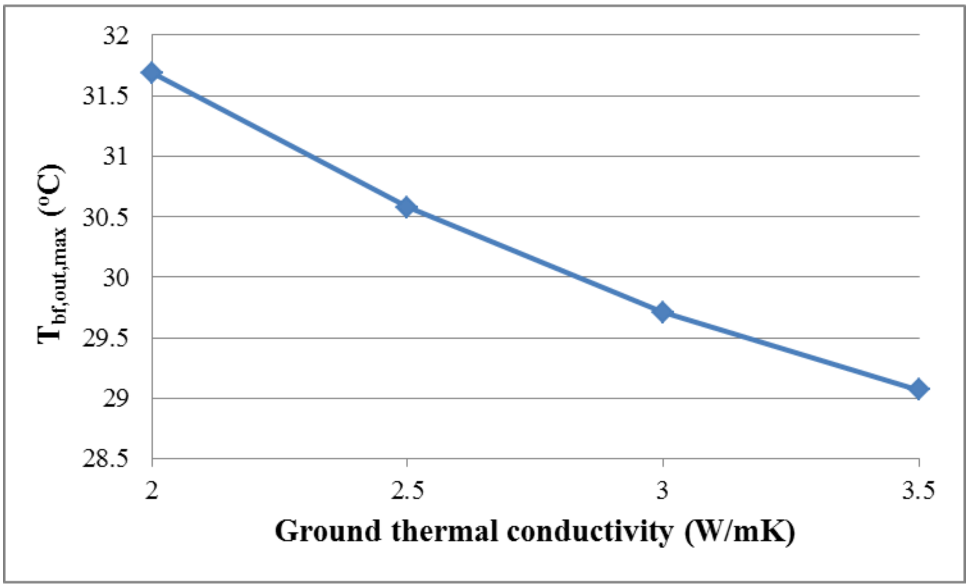

Fig. 4. Change of maximum borefield fluid leaving temperature against ground thermal conductivity for length of borehole at 140 m.

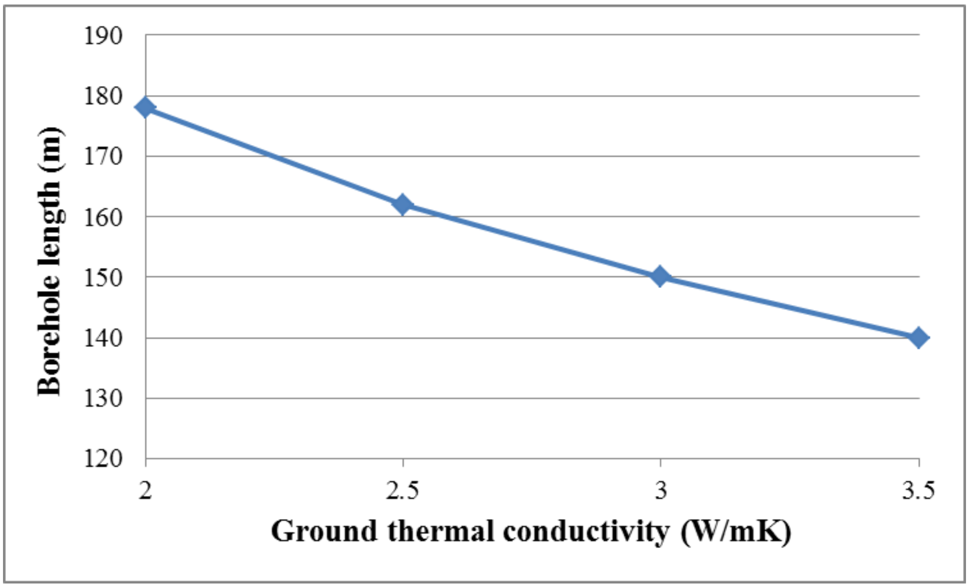

Fig. 5. Change of the required length of borehole against ground thermal conductivity for keeping maximum borefield fluid leaving temperature at 29 °C.

5.3 Effect of water heating demand on energy performance of RCHS

To provide drinking water for office use, the hot water demand was assumed to mainly take place at 9:00 a.m., 11:00 a.m., 13:00 p.m. or 15:00 p.m. with 200 mL of 100 °C hot water consumption per each occupant. This became 14.4 L/hour in total in a particular hot water demand period. The temperature of the potable make-up water was assumed to rise linearly from 15 to 25 °C from January to July and linearly drop back to 15 °C in December afterwards. Based on this demand profile, the simulated year-round primary energy consumption for the hot water system was 2,224 kWh without any solar assistance. Table 5 summarizes the year-round performances of the RCHS at different hot water consumption rates.

Table 5. Comparison of year-round performances of RCHS at different hot water consumption rates.

Hot water consumption rate (L/hour)	*SF*	$T_{zone,avg}$ (°C)	$RH_{zone,avg}$ (%)	Primary energy consumption (kWh)	Extra saving in primary energy consumption (kWh)
14.4 (design)	0.654	24.97	59.62	124,902	435
28.8 (2-fold)	0.648	24.97	59.62	127,558	1,003
72.0 (5-fold)	0.634	24.97	59.62	131,048	4,185
144 (10-fold)	0.613	24.97	59.65	139,917	6,436

From Table 5, it appears that the extra primary energy saving increased with the hot water consumption rate. In fact, even when the hot water consumption rate rose to 144 L/hour, that is ten times of the design hot water demand, it was still only 1.48% of the regenerative water flow rate (2.7 kg/s or 9,720 L/hour) required by the absorption chiller. Meanwhile, the energy consumption was just increased by 12.0%, showing that the effect of water heating demand was not as significant as that of cooling demand for office building application in the hot-humid region. The higher hot water consumption rate decreased the water temperature inside the hot water storage tank and the capacity of the absorption chiller. However, the averaged zone temperature and relative humidity were not much affected, since the ground-source radiant cooling had already provided most of sensible cooling to the building zone.

5.4 Analysis of annual profiles of system performances of RCHS

Fig. 6 depicts the annual profiles for the monthly total primary energy consumptions of the RCHS. The total primary energy consumption resembled similar trend as the primary energy consumption from the auxiliary heater which reached the maximum in June. Meanwhile, the primary energy consumption of electricity demand, which included that from the high-temperature chiller, pumps, fans and cooling tower, was the highest in July which followed the change of cooling load in a year. The discrepancy was due to the fact that the solar energy also achieved the peak during July.

As the primary energy consumption of auxiliary heating was associated with both the cooling demand and the availability of solar energy, the maximum demand for auxiliary heating was shifted to June. This could also be reflected by the variation of the monthly-averaged solar fraction as shown in Fig. 7. As seen, the profile for the monthly-averaged *SF* was simply the reverse of that for the monthly total primary energy consumption from the auxiliary heater.

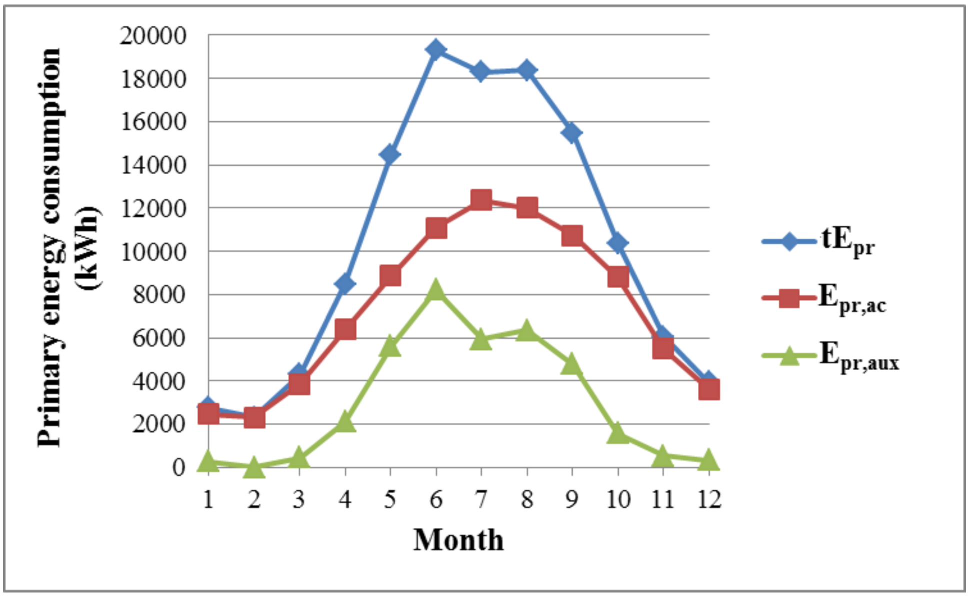

Fig. 6. Annual profiles of primary energy consumptions of RCHS.
(Abbreviation: tE_{pr}: total primary energy consumption of the entire system; $E_{pr,ac}$: primary energy consumption of electricity demand; $E_{pr,aux}$: primary energy consumption of auxiliary heating)

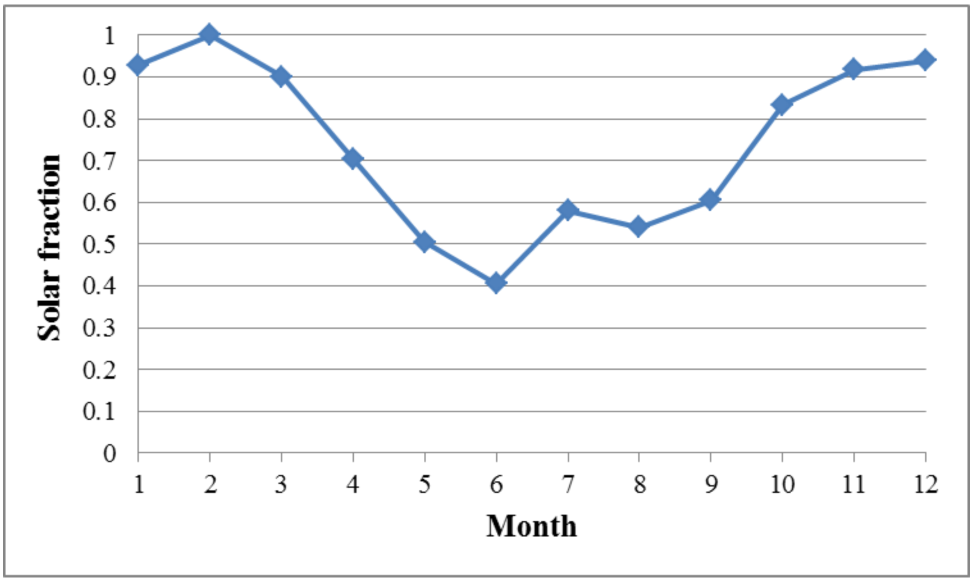

Fig. 7. Annual profiles of monthly averaged solar fraction of RCHS.

To deeply evaluate the performance of the RCHS, it was essential to know whether thermal comfort could be achieved. As such, the annual profiles of the indoor conditions were investigated. Fig. 8 describes the year-round profiles for the monthly-averaged zone temperature, while Fig. 9 for the zone relative humidity. It was found that T_{zone} was generally lower than the design temperature of 25.5 °C, while the RH_{zone} was around the design relative humidity of 60%. This showed that the RCHS could handle the zone sensible load well by using the high-temperature chiller, the radiant cooling and the absorption chiller under different operation modes throughout the year. Meanwhile, it tackled the zone latent load and ventilation load acceptably through the absorption chiller. As a result, the RCHS using PCB could provide satisfactory thermal comfort for the office building zone under appropriate modes of operation in different seasons.

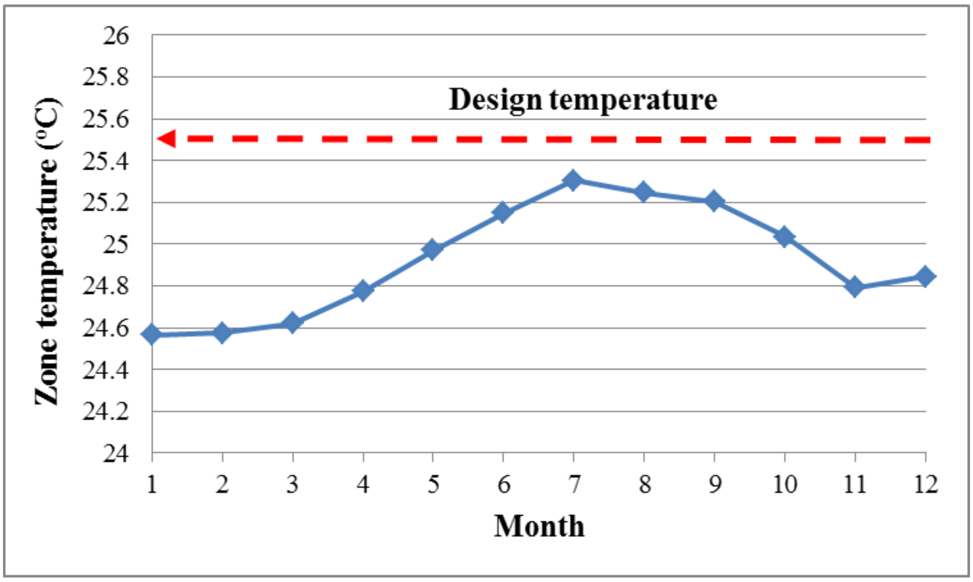

Fig. 8. Annual profiles of monthly averaged T_{zone} of the building zone.

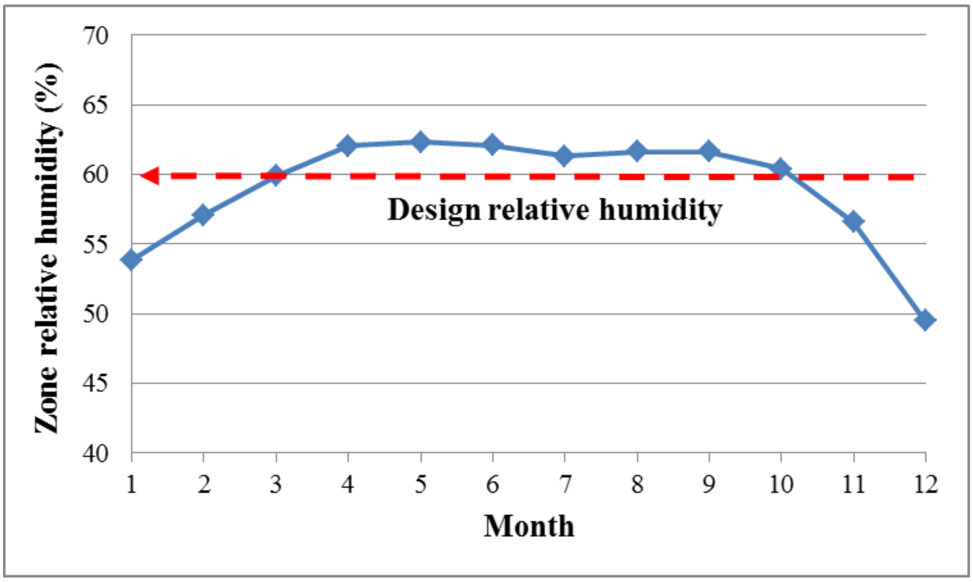

Fig. 9. Annual profiles of monthly averaged RH_{zone} of the building zone.

6. Conclusion and recommendation

A renewable cooling and heating system, which is featured with the hybrid use of renewable energy sources and the effective operation scheme, was developed to provide space cooling and water heating for building application in the hot-humid region. Solar energy was associated with absorption cooling for handling the ventilation load and zone latent load as well as water heating, while ground source was linked to radiant cooling through a high-temperature chiller for treating the zone sensible load in different occasions. Compared to the conventional air-conditioning, the RCHS using PCB could have 44.4% saving in year-round primary energy consumption with the zone temperature and relative humidity maintained close to the design levels. Through the parametric study, it was found that the ground property was critical for providing satisfactory year-round energy performance of the RCHS. To further enhance the paradigm of renewable cooling and heating, bioenergy can be included for auxiliary heating in the heat-driven absorption chiller, thus providing a more flexible cooling capacity for building application in the hot and humid climate. To cope with climate change mitigation, wider and deeper use of renewable energy is necessary in order to maintain low or even zero carbon urbanization.

Acknowledgement

This work described in this paper is fully supported by a grant from the Research Grants Council of the Hong Kong Special Administrative Region, China (Project No. CityU 123812).

Nomenclature

COP_{Ab}	Coefficient of performance of the absorption chiller
COP_{HTVCC}	Coefficient of performance of the high-temperature vapor-compression chiller
$E_{pr,ac}$	Primary energy consumption of electricity demand (kWh)
$E_{pr,aux}$	Primary energy consumption of auxiliary heating demand (kWh)
RH_{zone}	Zone relative humidity (%)
$RH_{zone,avg}$	Year-round-averaged zone relative humidity (%)
SF	Solar fraction
$T_{bf,out,max}$	Maximum borefield fluid leaving temperature (°C)
T_{zone}	Zone temperature (°C)
$T_{zone,avg}$	Year-round-averaged zone temperature (°C)
tE_{pr}	Total primary energy consumption of the entire system (kWh)

Abbreviations

BWP	Borefield Water Pump
CC	Chilled Ceiling
CWP	Cooling Water Pump
EWP	Chilled Water Pump
FCV	Free-Cooling Valve
GSHP	Ground-Source Heat Pump
GHE	Ground Heat Exchanger Borefield
HVAC	Heating, Ventilation and Air-conditioning
HWP	Hot Water Pump
PCB	Passive Chilled Beams

RCHS	Renewable Cooling and Heating System
RH	Relative Humidity
RPP	Radiant Panel Pump
RPV	Radiant Panel Valve
RWP	Regenerative Water Pump
SAF	Supply Air Fan
SAGSHP	Solar-Assisted Ground-Source Heat Pump
SAV	Supply Air Valve
WCVCC	Water-Cooled Vapor-Compression Chiller

References

2020-2030-2050 Common Vision for the Renewable Heating & Cooling Sector in Europe. European Technology Platform on Renewable Heating and Cooling, European Union, 2011.

Carrier Product Data, Active and Passive Chilled beams, Carrier Corporation, 2008.

Chan, A.L.S., Chow, T.T., Fong, S.K.F., Lin, J.Z., 2006. Generation of a typical meteorological year for Hong Kong. Energy Conversion and Management 47, 87-96.

Choi, J., Kang, B., Cho, H., 2014. Performance comparison between R22 and R744 solar-geothermal hybrid heat pumps according to heat source conditions. Renewable Energy 71, 414-424.

CIBSE TM51 Ground Source Heat Pumps. The Chartered Institution of Building Services Engineers London, 2013.

Common Implementation Roadmap for Renewable Heating and Cooling Technologies. European Technology Platform on Renewable Heating and Cooling, European Union, 2014.

Cui, Y., Wang, Y., Li, Z., 2015. Performance analysis on a building-integrated solar heating and cooling panel. Renewable Energy 74, 627-632.

Dai, L., Li, S., Liu, D., Li, X., Shang, Y., Dong, M., 2015. Experimental performance analysis of a solar assisted ground source heat pump system under different heating operation modes. Applied Thermal Engineering 75, 325-333.

De Carli, M., Galgaro, A., Pasqualetto, M., Zarrella, A., 2014. Energetic and economic aspects of a heating and cooling district in a mild climate based on closed loop ground source heat pump. Applied Thermal Engineering 71(2), 895-904.

Eicker, U., 2009. Low Energy Cooling for Sustainable Buildings. Wiley, Chichester.

Eicker, U., 2003. Solar Technologies for Buildings. Wiley, Chichester.

Eicker U., Pietruschka, D., Haag M., Schmitt, A., 2015. Systematic design and analysis of solar thermal cooling systems in different climates. Renewable Energy 80, 827-836.

Fong, K.F., Lee, C.K., Chow, T.T., 2012. Comparative study of solar cooling systems with building-integrated solar collectors for use in sub-tropical regions like Hong Kong. Applied Energy 90(1), 189-195.

Fong, K.F., Lee, C.K., Lin, Z., Chow, T.T., Chan, L.S., 2011. Application potential of solar air-conditioning systems for displacement ventilation. Energy and Buildings 43(9), 2068-2076.

Fong, K.F., Chow, T.T., Lee, C.K., Lin, Z., Chan, L.S., 2010a. Comparative study of different solar cooling systems for buildings in subtropical city. Solar Energy 84(2), 227-244.

Fong, K.F., Lee, C.K., Chow, T.T., Lin, Z., Chan, L.S., 2010b. Solar hybrid air-conditioning system for high temperature cooling in subtropical city, Renewable Energy 2010 35(11), 2439-2451.

Girard, A., Gago, E.J., Muneer, T., Caceres, G., 2015. Higher ground source heat pump COP in a residential building through the use of solar thermal collectors. Renewable Energy 80, 26-39.

Hang Y., Du, L., Qu, M., Peeta, S., 2013. Multi-objective optimization of integrated solar absorption cooling and heating systems for medium-sized office buildings. Renewable Energy 52, 67-78.

Henning, H-M., 2004. Solar-Assisted Air-Conditioning in Buildings. Springer-Verlag Wien, New York.

Hochschul Rapperswil of Switzerland, Test Report No. 264, 1997.

IPCC Special Report on Renewable Energy Sources and Climate Change Mitigation, Summary for Policymakers. Intergovernmental Panel on Climate Change, 2011.

Kavanaugh, S., Rafferty, K., 2014. Geothermal Heating and Cooling: Design of Ground-Source Heat Pump Systems. American Society of Heating, Refrigerating and Air-Conditioning Engineers, Inc., Atlanta.

Lee, C.K., Lam, H.N., 2008. Computer simulation of borehole ground heat exchangers for geothermal heat pump systems, Renewable Energy 33(6), 1286-1296.

Mehrpooya, M, Hemmatabady, H., Ahmadi, M.H., 2015. Optimization of performance of Combined Solar Collector-Geothermal Heat Pump Systems to supply thermal load needed for heating greenhouses. Energy Conversion and Management 97, 382-392.

Ozgener, O., Hepbasli, A., 2005. Performance analysis of a solar-assisted ground-source heat pump system for greenhouse heating: an experimental study. Building and Environment 40(8), 1040-1050.

Rad, F.M., Fung, A.S., Leong, W.H., 2013. Feasibility of combined solar thermal and ground source heat pump systems in cold climate, Canada. Energy and Buildings 61, 224-232.

Rosiek, S., Batlles, F.J., 2012. Shallow geothermal energy applied to a solar-assisted air-conditioning system in southern Spain: Two-year experience. Applied Energy 100, 267-276.

Safa, A.A., Fung A.S., Kumar, R., 2015. Heating and cooling performance characterisation of ground source heat pump system by testing and TRNSYS simulation. Renewable Energy 83, 565-575.

Si, Q., Okumiya, M., Zhang, X.S.,2014. Performance evaluation and optimization of a novel solar-ground source heat pump system. Energy and Buildings 70, 237-245.

TESS Library Documentation, Thermal Energy System Specialists, 2006.

TRNSYS 16, a TRaNsient SYstem Simulation program, the Solar Energy Laboratory, University of Wisconsin-Madison, 2006.

Verma, V., Murugesan, K., 2014. Optimization of solar assisted ground source heat pump system for space heating application by Taguchi method and utility concept. Energy and Buildings 82, 296-309.

Wang, E.Y., Fung, A.S., Qi, C.Y., Leong, W.H., 2012. Performance prediction of a hybrid solar ground-source heat pump system. Energy and Buildings 47, 600-611.

Yang, W.B., Sun, L.L., Chen, Y.P., 2015. Experimental investigations of the performance of a solar-ground source heat pump system operated in heating modes. Energy and Buildings 89, 97-111.